Optically measured diffusion constants of oxygen vacancies in MgO

Optically measured diffusion constants of oxygen vacancies in MgO

A Ueda[1,3]**, R Mu**[1]**, Y-S Tung**[1]**, M H Wu**[1]**, A Zavalin**[1]**, P W Wang**[2] **and D O Henderson**[1]

[1] Chemical Physics Laboratory, Department of Physics, Fisk University, Nashville, TN 37208, USA
[2] Department of Physics, The University of Texas at El Paso, El Paso, TX 79968, USA

E-mail: aueda@fisk.edu

Abstract
We report the estimation of diffusion constants for oxygen vacancies in MgO based on optical absorption spectra. MgO single crystals were annealed in a reducing atmosphere (H_2 + Ar) to create oxygen vacancies and the samples were annealed in an oxidizing atmosphere (O_2 + Ar) to annihilate them. Fe^{3+} impurities in the MgO samples were utilized to monitor the degree of reduction or oxidation of the samples during the annealing cycle. An activation energy of 3.08 eV for the diffusion of oxygen vacancies (F-centres) in MgO was obtained, based on the absorption measurements of Fe^{3+} band.

1. Introduction

Since MgO is relatively insoluble, hard, durable, and transparent in the range between 350 and 7000 nm, it is a material widely used in optics. The optical absorption edge of MgO with a low impurity concentration is ∼7.8 eV (160 nm) [1]. Fe^{3+} is a common impurity in MgO, and its absorption bands are found at 210 and 285 nm [1]. It has been reported that the bands at 248 and 252 nm are attributed to F-centres and F^+-centres, respectively [2]. The F-centre is defined as an oxygen vacancy with two trapped electrons, while the F^+-centre is defined as an oxygen vacancy with one electron. In this paper, we may use the words 'oxygen vacancies' as having an equivalent meaning to F-type (F-, F^+-, and F^{2+}-) centres. Oxygen vacancies can be created by neutron, ion, photon or electron irradiation or Mg vapour deposition at high temperature (the so called *additively coloured crystal*) [2]. Bands located at 250, ∼355, ∼575, and 975 nm caused by irradiation can be annealed out at 600 °C, while the bands generated by Mg vapour deposition are not annealed out until the annealing temperature reaches the region of 1000–1200 °C [2]. The explanation for this is as follows: in the irradiated samples oxygen vacancies are generated by a knock-on process or electronic excitation, and at the same time oxygen interstitials are created. The interstitial oxygen becomes mobile at a relatively low temperature (<600 °C), allowing most oxygen vacancies to recombine with these interstitials.

[3] Contact author.

On the other hand, in the additively coloured samples, excessive Mg^{2+} ions are introduced from Mg vapour at 1800 °C, and the Mg^{2+} ions migrate into the MgO bulk yielding oxygen ion vacancies. In this case there exist no oxygen interstitials in the system, and oxygen vacancies are not mobile at temperatures below 900 °C. Accordingly, these oxygen vacancies cannot be annealed out below 900 °C [2]. The creation of oxygen vacancies by annealing in a reducing atmosphere represents the same situation as in the case of additively coloured MgO, in the sense that there are no oxygen interstitials formed during the creation of oxygen vacancies. Instead of introducing excessive Mg^{2+} ions into the system, oxygen ions are removed from the system by annealing the sample in a reducing atmosphere. In this paper, we report: (i) the correlation between the reduction of Fe^{3+} and the creation of oxygen vacancies and (ii) the estimation of diffusion constants of oxygen vacancies by utilizing intensity changes in the impurity Fe^{3+} band. This approach represents a method for estimating diffusion coefficients for oxygen vacancies that lack clearly defined absorption features in the UV-Vis range from which to obtain diffusion coefficients and an activation energy.

2. Experimental details

MgO single crystals (15 mm × 15 mm × 0.5 mm) oriented ⟨100⟩ were obtained from Harrick Scientific. The major impurities are Fe^{3+} (∼100 ppm) and Al^{3+} (∼40 ppm). The electronic spectra were measured between 185–3200 nm with a UV-Vis-NIR double beam spectrophotometer (Hitachi, U-3501). Thermal annealing was carried out in a tube furnace at temperatures between RT and 1300 °C in a reducing (10% H_2 + 90% Ar) and an oxidizing (10% O_2 + 90% Ar) atmosphere.

3. Experimental results

3.1. Transmission of Fe^{3+} band in MgO for monitoring of reduction of MgO

The transmission spectrum of the MgO sample before annealing is shown in figure 1. The sample has a high transmittance in the 350–3200 nm region. There is a 15% loss mainly due to the reflection at the front and back surfaces ($R = (n - 1)^2/(n + 1)^2 = 0.073$, where $n = 1.74$). Below 320 nm, the transmittance suddenly drops, mainly due to absorption by Fe^{3+} ion impurities located at 285 and 210 nm.

Figure 2(a) shows the spectra of MgO annealed in the reducing atmosphere. Spectrum (a) is the transmittance for MgO before annealing. Spectra (b), (c), and (d) are for the same sample after sequential annealing at 1000, 1100 and 1200 °C, respectively, for 15 min each. Spectra (e) to (i) are for the same sample additionally annealed at 1200 °C for the total annealing times of 30, 45, 60, 75 and 90 min, respectively. During annealing between 200 and 900 °C in steps of 100 °C for 15 min, the spectra did not exhibit any significant changes (they are not shown in the figure). After annealing at 1200 °C for a total of 90 min, (i) of figure 2(a), the surface of the sample became slightly cloudy, causing a decrease of transmission due to the scattering. However, before the sample became cloudy, the Fe^{3+} band at 285 nm became weaker and this resulted in an increased transmittance to ∼60% at 285 nm. This indicates that the Fe^{3+} ions were reduced to Fe^{2+} ions in the reducing atmosphere at high temperature [3]. After annealing in the reducing atmosphere, the sample was subsequently annealed in an O_2 + Ar atmosphere. The transmittance suddenly dropped to ∼10% at 285 nm just after annealing at 1200 °C in the oxidizing atmosphere for 15 minutes, as shown in figure 2(b).
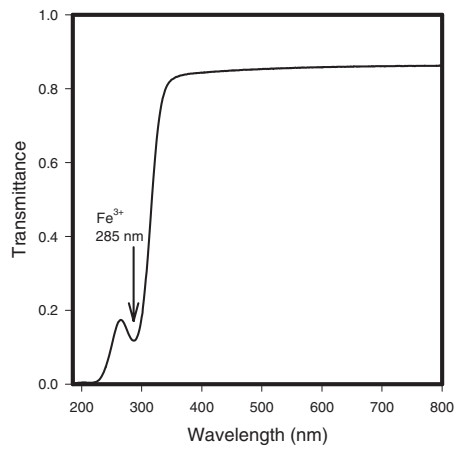
**Figure 1.** Transmission spectra of single crystal MgO without any thermal treatment.
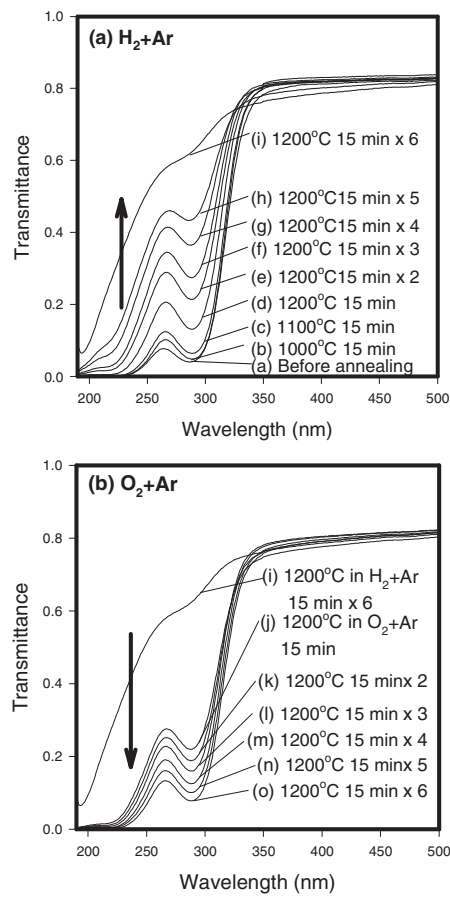
Figure 2. Transmission spectrum of MgO annealed in (a) H_2 + Ar and (b) O_2 + Ar in the range of the Fe^{3+} absorption band.

3.2. Annealing temperature dependence of Fe^{3+} bands

A single MgO crystal was annealed at 1200 °C in O_2 + Ar atmosphere for 5 h to prepare a starting sample (the sample state O). The sample was then annealed in the reducing atmosphere for 5 h and transmission spectra were obtained at each temperature from 400 to 1300 °C in steps of 100 °C to evaluate the degree of reduction as a function of annealing temperature. The sample annealed at 1300 °C in the reducing atmosphere for 5 h is referred to as the sample state R. The sample (state R) was subsequently annealed in an oxidizing atmosphere for 5 h at each temperature from 400 to 1300 °C. This measurement is similar to the results shown in figure 2, however the annealing time and temperatures are different.

The area under the Fe^{3+} absorption band at 285 nm was integrated for each temperature from RT (25 °C) to 1300 °C. In figure 3, the annealing temperature dependence of the Fe^{3+} band is plotted for the samples annealed in both reducing and oxidizing atmospheres. Trace (1) shows the integrated band intensity as a function of annealing temperature in the reducing atmosphere starting with the sample state O. The integrated intensity of the Fe^{3+} band did not change until the annealing temperature reached 900 °C. At this temperature, Fe^{3+} started to be reduced to Fe^{2+}. The reduction of Fe^{3+} then indicates the creation of oxygen vacancies, as we will show. The band completely disappeared at 1300 °C. This sample (sample state R) was used as the starting sample for annealing in the oxidizing atmosphere. Trace (2) shows that the Fe^{3+} band did not appear until the annealing temperature reached 900 °C, and at 1000 °C the sample started to be oxidized. The Fe^{3+} absorption band completely recovered at 1300 °C.
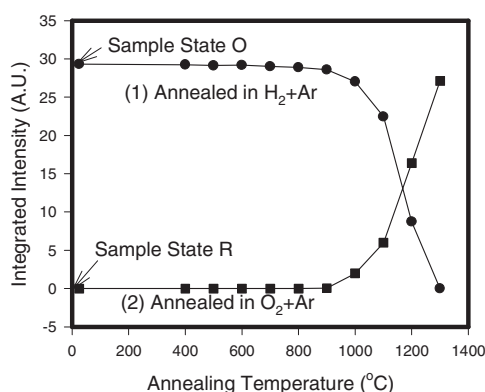
Figure 3. Annealing temperature dependence of the Fe^{3+} band in (1) H_2 + Ar and (2) O_2 + Ar. The starting sample for (1) was the oxidized state O, and that for (2) was the reduced state R.

3.3. Correlation between Fe^{3+} band and F_n-band at 575 nm

After annealing the sample (state O) in the reducing atmosphere, an absorption band developed at 575 nm. Figure 4 shows the temperature dependence of the Fe^{3+} and 575 nm bands. The intensity of the Fe^{3+} decreased as the annealing temperature increased, while the absorption at 575 nm increased. The band at 575 nm has been observed previously for MgO irradiated with neutrons and ions [2, 4, 5], and was attributed to aggregates of F-centres. Therefore, the correlation between the reduction of Fe^{3+} and the development of the 575 nm band suggests that the reduction of Fe^{3+} coincides with the creation of F-centres. Figure 4(b) shows the temperature dependence of the 575 nm band.
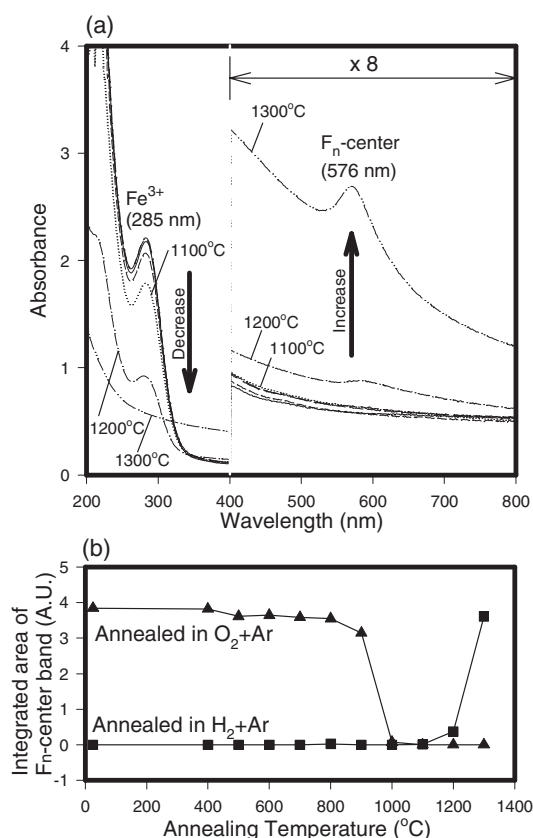
Figure 4. (a) The temperature dependence of the Fe^{3+} and 575 nm bands during annealing in the reducing atmosphere. The Fe^{3+} band decreased as the annealing temperature increased, while the 575 nm band developed. (The vertical scale is magnified in the range 400–800 nm by a factor of 8.) (b) Integrated area of the 575 nm band as a function of annealing temperature for the cases of annealing in O_2 + Ar and H_2 + Ar.

4. Discussion

The intensity of the Fe^{3+} absorption band depends strongly on the annealing atmosphere. Although the F-type (F- and F$^+$-) centre bands near 250 nm were not directly measured, the Fe^{3+} impurity band was used to monitor the state of MgO that is correlated to the creation or annihilation of F-type centre bands.

4.1. The reversible conversion between Fe^{3+} and Fe^{2+}

The Fe^{3+} impurities are incorporated into the MgO lattice as a complex of Fe_2O_3 [4]. In MgO, the Fe^{3+} ion has a lower energy than the Fe^{2+} ion, through a Hubbard-type interaction [5]. Thus, the iron impurity takes the ion state of Fe^{3+} in MgO under the normal conditions. However, if there exists an electron donor nearby, or the sample is annealed in a reducing atmosphere, Fe^{3+} can be reduced to the ferrous ion Fe^{2+} [3].

In the reducing atmosphere at high temperature, the following chemical reactions occur at the MgO surface: a hydrogen molecule reacts with an oxygen ion at the MgO surface to

form a water molecule, and leaves behind an oxygen vacancy with two electrons [3]:

$$H_2 + O^{2-} \longrightarrow H_2O + [O_{vac}] + 2e^- \tag{1}$$

where $[O_{vac}]$ represents an oxygen vacancy without electrons. Under thermodynamic equilibrium, this reaction would not be expected to occur, because the free energy change ΔG is positive. However, under non-equilibrium conditions imposed by a flowing dry hydrogen atmosphere, the reaction can occur and is promoted by the removal of water [3]. The system $([O_{vac}] + 2e^-)$ is an F-centre. An F-centre, once created, can transfer one electron to an Fe^{3+} ion to form an Fe^{2+} ion [3]:

$$Fe^{3+} + ([O_{vac}] + 2e^-) \longrightarrow Fe^{2+} + ([O_{vac}] + e^-). \tag{2}$$
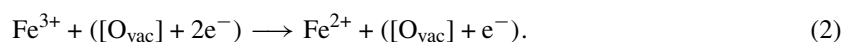
In this case, the system $([O_{vac}] + 2e^-)$ becomes $([O_{vac}] + e^-)$, which is an F^+-centre.

According to Grigg's experiments, annealing MgO samples in reducing atmospheres demonstrated that the reducing gas used for the annealing did not diffuse into the sample [3]. At high temperatures ($\geqslant 900\,^\circ C$), annealing in the reducing atmosphere causes the diffusion of F-type centres (F-, F^+-, and F^{2+}-centres) into the sample, because the creation of F-type centres at the surface results in a concentration gradient of oxygen vacancies. The diffusion of F-type centres into the sample implies that oxygen ions diffuse to the surface and ultimately diffuse out from the sample through the reducing reaction in equation (1). At a lower temperature ($<900\,^\circ C$), the reaction will not proceed, because oxygen vacancies are not mobile [2].

When annealing the samples in the oxidizing atmosphere at high temperature ($>900\,^\circ C$), the conversion from Fe^{2+} to Fe^{3+} takes place, as shown by trace (2) in figure 3. We can expect that, at the surface, an oxygen vacancy with two electrons will be filled with an oxygen atom to become an oxygen ion O^{2-}, where the atomic oxygen is created at Mg-rich (oxygen-deficient) surfaces of MgO from molecular oxygen as the Mg-rich surface has a tendency to be oxidized:

$$O_2 + Mg \longrightarrow MgO + O \tag{3a}$$

$$([O_{vac}] + 2e^-) + O \longrightarrow O^{2-}. \tag{3b}$$

If there is an Fe^{2+} near an F^+-centre, the oxygen atom can accept an electron from Fe^{2+} to convert it to Fe^{3+}, and the oxygen atom becomes an oxygen ion:

$$([O_{vac}] + e^-) + Fe^{2+} + O \longrightarrow Fe^{3+} + O^{2-}. \tag{4}$$
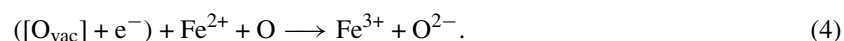
The processes of Fe reduction (equation (2)) and oxidation (equation (4)) are completely reversible.

4.2. Diffusion of oxygen vacancies

The diffusion constants were estimated for oxygen vacancies from the transmission data of MgO annealed in the reducing atmosphere for 5 h at each temperature. For the estimation of the diffusion constants, it is assumed that Fe^{3+} ions are uniformly distributed in the virgin MgO sample with a concentration on the order of 100 ppm before annealing. It is also assumed that the diffusion constants of F-centres are similar to F^+-centres, although the electronic states of these centres are expected to cause some differences between the F- and F^+-centres in the diffusion processes. Kotomin *et al* theoretically calculated that the activation energies for the diffusion of F^+- and F-centres were 2.72 eV and 3.13 eV, respectively [8]. In this work, the diffusion constants were obtained from the integrated areas of the absorption due to Fe^{3+} ~285 nm for temperatures from 800 to 1200 $^\circ C$. Below 700 $^\circ C$ there were not any significant changes, and the data below 700 $^\circ C$ are not appropriate for estimating the

diffusion constants. The ratio of the integrated absorbance at each temperature to that at RT is proportional to the amount of the Fe^{3+} present in the sample at each temperature. Figure 5(a) schematically shows that the concentration of Fe^{3+} ions is decreased from both surfaces due to the reduction. The concentration curve should follow a differential equation of diffusion with suitable boundary conditions that include the rate equation of the chemical reactions at both the surfaces. However, the concentration change resulting from the reduction of Fe^{3+} to Fe^{2+} was simplified as there was a sharp boundary between Fe^{3+} and Fe^{2+} domains. Figure 5(b) illustrates that the remaining amount of the Fe^{3+} in the sample is proportional to the thickness of the layer $(d - 2x)$ containing Fe^{3+}, where d is the sample thickness of 0.5 mm and x is the approximate thickness of the layer (the diffusion length) in which Fe^{3+} ions are converted to Fe^{2+}. Therefore, the ratio of the integrated absorbance at each temperature to that at RT (A/A_0) can be related to the diffusion length x:

$$\frac{(d - 2x)}{d} = \frac{A}{A_0} \qquad (5)$$

where A is the integrated value of the absorption band due to Fe^{3+} in the sample annealed at a certain temperature T and A_0 is that for the sample at state O. The effect of the diffusion from the crystal edges is neglected for this estimation. On the other hand, the diffusion constants of the oxygen vacancy can be described by the following equation, according to Fick's law [9]:
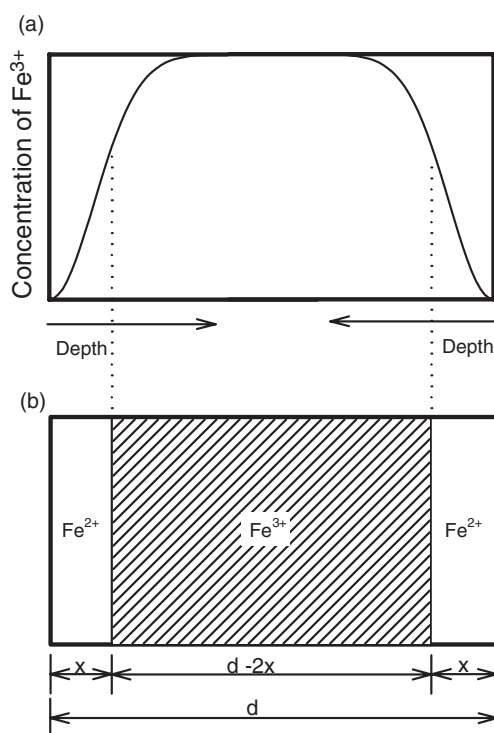
Figure 5. Schematics of (a) Fe^{3+} concentration in the MgO sample during annealing in the reducing atmosphere and (b) the parameters used for the estimation of the diffusion constants.
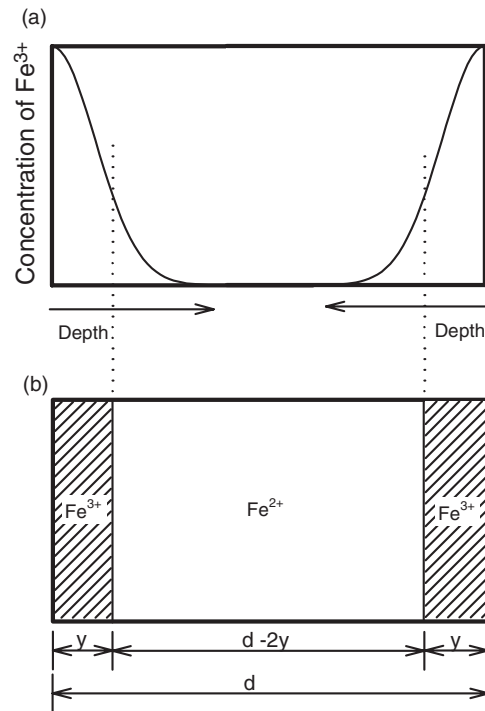
Figure 6. Schematics of (a) Fe^{3+} concentration in the MgO sample during annealing in the oxidizing atmosphere and (b) the parameters used for the estimation of the diffusion constants.

$$D = D_0 \exp\left(-\frac{E_a}{k_B T}\right) \tag{6}$$

where E_a is the activation energy for the diffusion of oxygen vacancies, k_B is the Boltzmann constant, T the absolute temperature, and D_0 is the pre-exponential factor [9]. The diffusion length during a diffusion time t is given by

$$x = (Dt)^{1/2} = (D_0 t)^{1/2} \exp\left(-\frac{E_a}{2k_B T}\right) \tag{7}$$

Combining this equation with equation (5), we obtain the relationship between the experimental absorption data and the activation energy E_a for the diffusion of oxygen vacancies:

$$x = \frac{d}{2}\left(1 - \frac{A}{A_0}\right) = (D_0 t)^{1/2} \exp\left(-\frac{E_a}{2k_B T}\right). \tag{8}$$

For the case of annealing in the oxidizing atmosphere, the reverse process is expected. Therefore, annealing of the reduced sample in the oxidizing atmosphere causes oxidation of the layer containing Fe^{2+} from the surfaces as shown in figure 6. In this case, the ratio (A/A_0) of the integrated absorbance at each temperature to that of sample state O can be related to the diffusion length y:

$$\frac{2y}{d} = \frac{A}{A_0}. \tag{9}$$

From this equation and equation (6), the diffusion length can be related to the diffusion constants as follows, instead of equation (8):

$$y = \frac{d}{2}\left(\frac{A}{A_0}\right) = (D_0 t)^{1/2} \exp\left(-\frac{E_a}{2k_B T}\right). \tag{10}$$
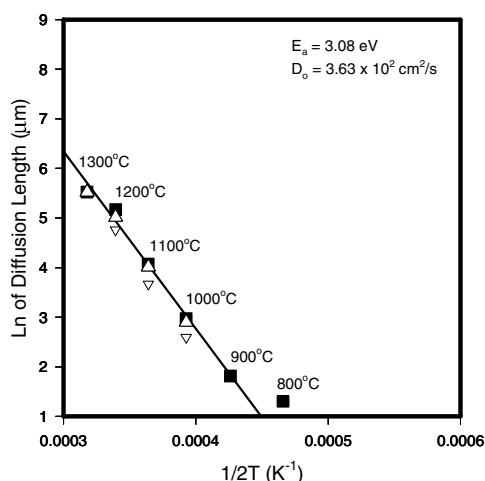
Figure 7. Linear fitting for the estimation of diffusion constants. The full square symbol is for annealing in the reducing atmosphere, the open triangle is for the oxidizing atmosphere, and the inverted open triangle is from another set of data for the reducing atmosphere.
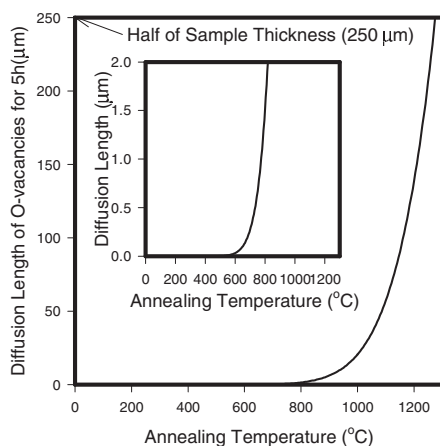
Figure 8. The diffusion length of oxygen vacancies as a function of annealing temperature for 5 h, using the values of the diffusion coefficient and the activation energy obtained from this study.

Taking the logarithm of both sides of equations (8) and (10), we plotted these quantities versus $1/2T$ to obtain the values of E_a and D_0, as shown in figure 7. A linear fitting of the plot gave values of $E_a = 3.08 \pm 0.18$ eV and $D_0 = 3.63 \times 10^{10} \, \mu\text{m}^2 \, \text{s}^{-1}$ (because of accumulated data, this value is more reliable than the previously reported value ($E_a = 3.32$ eV) in [10]). The value of the activation energy is between the values for F^+- and F-centres (2.72 eV and 3.13 eV, respectively) that Kotomin *et al* theoretically calculated [8]. Using these experimental values ($E_a = 3.08$ eV and $D_0 = 3.63 \times 10^{10} \, \mu\text{m}^2 \, \text{s}^{-1}$), the diffusion length for 5 h was re-calculated and plotted as a function of temperature, as shown in figure 8. In the inset, the vertical scale is magnified to reveal the small change at lower temperature. According to the plot, the diffusion length of oxygen vacancies reaches about 1 μm at 800 °C for 5 h. Macroscopically, oxygen vacancies start to diffuse into the sample at around 900 °C. This is consistent with the results by Chen *et al* that the oxygen vacancies in MgO become mobile near 900 °C [2].

5. Conclusions

We have reported the experimental estimation of diffusion constants for oxygen vacancies in MgO. MgO single crystals were annealed in a reducing atmosphere (H_2 + Ar) to create oxygen vacancies. Fe^{3+} impurities in MgO samples were used as a probe to monitor the degree of reduction or oxidation of the samples due to annealing. From the absorption measurements of Fe^{3+} band, the diffusion constant and activation energy of oxygen vacancies in MgO were obtained to be $E_a = 3.08$ eV and $D_0 = 3.63 \times 10^{10}$ μm^2 s^{-1}. The activation energy of 3.08 eV is in reasonable agreement with the theoretical calculations of Kotomin *et al* [8].

Acknowledgments

References

[1] Williams R T 1986 Radiation Damage *Handbook of Laser Science and Technology* ed M J Weber (Boca Raton, Florida: CRC Press) section 2
[2] Chen Y, Williams R T and Sibley W A 1969 *Phys. Rev.* **182** 960
[3] Briggs A J 1975 *Mater. Sci.* **10** 737
[4] Henderson B and Bowen D H 1971 *J. Phys. C: Solid State Phys.* **4** 1487
[5] Evans B D, Comas J and Malmberg P R 1972 *Phys. Rev.* B **6** 2453
[6] Yager T A and Kingery W D 1981 *J. Mater. Sci.* **16** 483
Yager T A and Kingery W D 1981 *J. Mater. Sci.* **16** 489
[7] Timmer G and Borstel G 1991 *Phys. Rev.* B **43** 5098
[8] Kotomin E A, Kuklia M M, Eglitis R I and Popov A I 1996 *Mater. Sci. Engng* B **37** 212
[9] Kittel C *Introduction to Solid State Physics* (New York: Wiley)
[10] Ueda A *et al* 1998 *Nucl. Instrum. Methods* B **141** 261